Cellulose (2016) 23:3393–3398
DOI 10.1007/s10570-016-1044-5

COMMUNICATION

High velocity dry spinning of nanofibrillated cellulose (CNF) filaments on an adhesion controlled surface with low friction

Yingfeng Shen · Hannes Orelma · Asko Sneck · Kirsi Kataja · Juha Salmela · Pia Qvintus · Anna Suurnäkki · Ali Harlin

Received: 17 May 2016 / Accepted: 13 August 2016 / Published online: 19 August 2016

Abstract A new process for preparing thin cellulose nanofibril (CNF) filaments (thickness of 16 μm) was investigated by utilizing the dry spinning approach. In the process, CNF hydrogel was extruded through a fine nozzle onto an adhesion controlled capstan (drum) with low friction (slippery surface) at a speed of up to 11 m/s. The utilized capstan enables excellent line speed control when the slippery surface is applied, and prevents drying shrinkage of the spun filaments. The mechanical properties of prepared filaments can be optimized with the stretch ratio, the ratio of the speed of the drum surface, and the CNF jet flow. The developed method allows for manufacturing thin CNF filaments with an elevated spinning rate in a more controlled manner.

Keywords CNF · Filament · Spinning · Dry-spinning · SEM · Tensile strength

Electronic supplementary material The online version of this article (doi:10.1007/s10570-016-1044-5) contains supplementary material, which is available to authorized users.

Y. Shen · H. Orelma (✉) · A. Sneck · K. Kataja · J. Salmela · P. Qvintus · A. Suurnäkki · A. Harlin
VTT, Technical Research Centre of Finland, Biologinkuja 7, P.O. Box 1000, 02044 Espoo, Finland
e-mail: hannes.orelma@vtt.fi

Present Address:
J. Salmela
Spinnova Ltd, Vaajakoski, Finland

Introduction

Currently, the textile and composite industries are searching for greener filaments made from renewable resources to compensate for the use of synthetic oil-based materials. Wood-based cellulose is one of the biomaterials with the highest potential and which has already been utilized in a wide range of textile filaments for decades (Cook 1984). It is a fully renewable material and exhibits excellent characteristics for filament and yarn manufacturing e.g. availability, biodegradability, easy modifiability, and low price.

The length of wood fibers [as an example: length of spruce fibers is 3.4 mm (Klemm 1998)] limits the utilization of typical mechanical manufacturing methods, including carding, which is usable with long fiber materials. The dissolution with solvent coagulation has, therefore, been the dominating industrial route to producing wood-based textile filaments (Cellulose II filaments) such as viscose fibers. Due to the environmental toxicity of current dissolution chemicals, the novel filaments from mechanically disintegrated cellulose nanofibril (CNF) have achieved more attention.

Cellulose nanofibrils (CNFs) belong to the group of green high-strength cellulosic materials (Eichhorn et al. 2010). Its good mechanical properties have already been utilized in various applications, including films (Syverud and Stenius 2009), aerogels (Paakko et al. 2008), and rheology modification (Turbak et al. 1983). It has also been reported that strong filaments

(tensile strengths up to 320 MPa) can be obtained from CNF by means of solvent coagulation (Walther et al. 2011; Iwamoto et al. 2011). Moreover, by controlling the manufacturing conditions, the mechanical properties of the filaments can be further tuned. The fibril orientation in CNF filaments correlate with the filament strength, as has recently been shown by Håkansson et al. (2014) who produced CNF filaments with tensile strength above 500 MPa by means of a specific nozzle design. A drawback of the reported liquid coagulation method is the uncontrolled removal of water from the structure of the wet CNF filament, which leads to shrinking of the filament's cross sectional profile and may leave the filament hollow. Moreover, the current wet-spinning technology sets limits for the maximum spin rate applicable with the spinning process.

In the present work, we have developed a method to avoid both uncontrolled removal of water and the spinning rate limitation by utilizing dry spinning using an adhesion controlled surface with low friction (slippery surface). The dry spinning approach has already been utilized with banana rachis CNF (Hooshmand et al. 2015). In the given method the filament is slowly spun into air without shrinkage control. In our method, CNF filaments are directly spun on a capstan, enabling excellent line speed control when applying the slippery surface, eliminating the need for the coagulation bath and shrinkage control (Fig. 1). The oiled surface layer acts as a low friction surface and non-adhering layer (Quéré 2011). This eliminates a need of shrinkage control allowing the wet CNF filament to dry in a more controllable manner. By infusing a porous surface with lubricating fluid, a very low contact angle hysteresis (<2.5°) can be obtained (Wong et al. 2011). Such a low contact angle hysteresis allows a meniscus of the wet ribbon to reach its equilibrium contact angle also when a dense gel such as a CNF hydrogel is utilized. Therefore, it was expected that the non-adhering surface approach allows for maintaining the cross-sectional shape of the filament during drying.

The utilization of a solid capstan (drum) instead of the coagulation bath also opens new venues for controlling the fibril orientation of the spun filament. In the traditional wet spinning approach, the fibril orientation is achieved inside the nozzle by hydrodynamic forces. In the dry-spinning approach, however, the filament orientation can be further tuned by means of the speed ratio between the CNF feed and the rotation speed of the collector capstan. The introduced new setup allows both stretching and squeezing of the filament, which widens the controllability of the spinning process. This phenomenon can be utilized

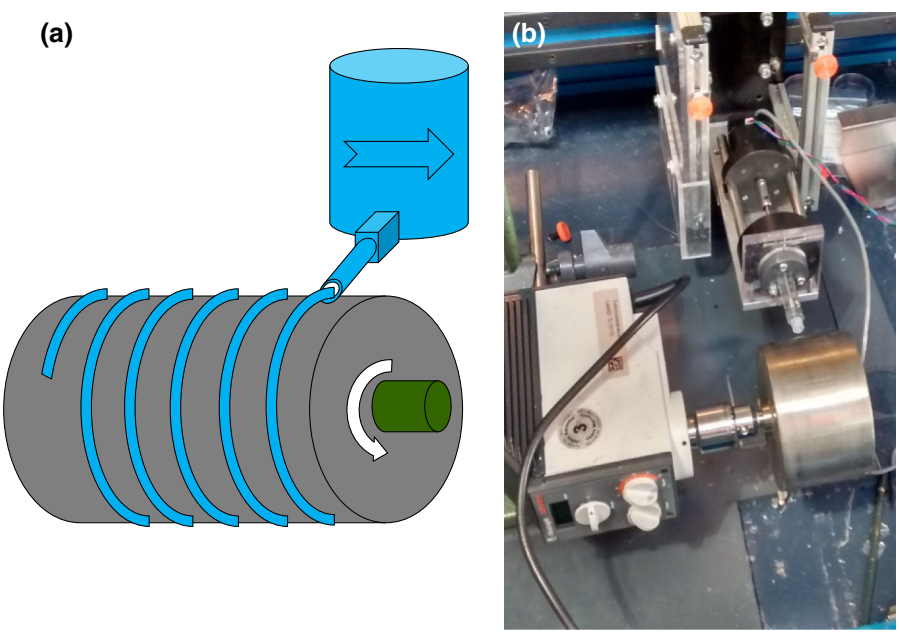

Fig. 1 **a** Schematic illustration of the dry-spinning concept. **b** The lab size instrumentation utilized in the study

to optimize the orientation of the CNF filament for maximizing the filament's strength profile. The developed method is easily up-scalable for the industrial manufacturing of CNF filaments.

Materials and methods

Nanofibrillated cellulose (CNF)

The raw material of the CNF filaments was bleached birch Kraft pulp with and without alkaline TEMPO–NaBr–NaClO oxidation (Isogai and Kato 1998). Both pulps were first grinded once with a Masuko grinder. The grinded unmodified and TEMPO-oxidized pulps were then passed six times and one time only, respectively, through the microfluidizer Microfluidics M-110EH (Westwood, USA), equipped with a chamber pair (Chambers 200 and 100 μm). The resulting CNF gels had a solid content of 1.64 wt%. In the case of the unmodified CNF, the gel was further concentrated to 3 wt% using centrifugation. The charge density of the TEMPO-CNF was 1.1 meq/g and the solid content of the gel was diluted to 0.819 wt% with the assistance of mild tip-sonification. The shear thinning behavior of TEMPO-CNF gel was measured with a rotary rheometer (Figure S1, supporting information).

Preparation of low friction surface (slippery surface)

A polyethylene (PE) coated aluminum capstan was used as a carrier substrate for the CNF filaments. The polyethylene film was tightly wrapped on a rotating capstan so as to remove the roughness of the capstan. The low friction surface was prepared on the PE-foil by applying sunflower oil with a brush while the capstan was rotating. The volume of the applied oil layer was estimated to be 1–3 g/m^2 and the respective layer thickness between 1 and 3 μm.

Wet extrusion of nanofibrillated cellulose

The schematic illustration and a photo image of the extrusion system are shown in Fig. 1a, b. A custom-made extruder was used to pass the CNF hydrogel through a syringe needle. The inner diameter and length of the needle were 108 μm and 8 mm, respectively. The extruder was horizontally mounted on the z-axis of a CNC machine and controlled as the 4th axis with EMC2 software, which can control both the x–y–z motion and the extruder. The speed of the jet coming out from the nozzle can vary from 4 to 32 m/s. A rotating capstan was driven horizontally by a Heidolp RZR 2021 overhead laboratory stirrer with a rotation speed accuracy of 1 RPM. The diameter of the capstan was 104 mm and the width 70 mm. By adjusting the speed of the motor, the surface speed of the capstan (drum) can vary by 2–11 m/s, which is also the speed of the filament production. The stretch ratio was calculated by the Eq. (1).

$$\textit{Stretch ratio}\,(\lambda) = \frac{\textit{Surface speed}\,(\mathrm{m/s})}{\textit{Jet speed}\,(\mathrm{m/s})} \qquad (1)$$

In a typical experiment, the oil coating was first applied onto the polyethylene film on the rotating capstan with the rotating speed of 11 m/s. Then the jet was started and a wet CNF filament was collected for a couple of seconds to clear the nozzle and to raise the pressure in the extruder. Then the nozzle moved linearly along the capstan with a constant move rate. The horizontal move speed was selected so that no over lapping between neighboring filament rounds took place. Finally, after collecting a 10 m filament the capstan continued rotating at room temperature for 3 min to dry the filament. Then the dried filament was removed from the capstan.

SEM-imaging of filaments

The filament topography was investigated using a Zeiss Merlin Field-Emission SEM. For cross-sectional analysis, the filaments were freeze-fractured under liquid nitrogen at atmospheric pressure. For surface analysis, the filaments were secured on a sample stub with a carbon tape. In both cases the samples were coated with a thin layer of platinum using a sputter coater. The SEM was operated using 2 kV acceleration voltage, utilizing both secondary electron and In-Lens SE detectors.

Tensile testing of filaments

The strength of the dry-spun filaments was measured with a universal testing machine (custom made tensile tester utilizing a 4-digit Precisa balance to measure the

tension force). The force was monitored at 10 Hz through serial communication with a PC and the maximum force before the filament break was then used to calculate the tensile strength. The tensile tests were carried out with a span length of 30 mm and the speed of 3 mm/min with a geared stepper motor.

The cross-sectional area of the dry-spun CNF filament was estimated by weighing and utilizing the bulk density of dry CNF 1.5 g/cm^3 (Nogi et al. 2009; Håkansson et al. 2014). The calculated values were verified by comparison with the cross-sectional images taken by the SEM and with calculated estimations from the used spinning parameters: the solids content of the hydrogel, extrusion speed, and surface speed. The samples were kept in 50 % relative humidity at 25 °C for 12 h, and then the tensile strength measurements were carried out under the same conditions. At least seven parallel measurements were carried out in order to obtain standard deviations.

Results

CNF filament spinning on a rotating capstan with non-adhesive coating

The CNF dry-spinning studies were started by evaluating first the effect of the applied oil layer on the spinnability of unmodified CNF. The flow rate of the jet compared to the capstan surface velocity (surface velocity of the capstan was 11 m/s) was fixed to the ratio of 1, where no stretching or squeezing took place.

It was found that the oil layer was mandatory for achieving a uniform CNF filament. Without the oil layer the CNF filament collapsed to a film shape when dried due to the strong adhesion forces between the CNF ribbon and the polyethylene foil (Figure S2, supporting information). The strong adhesion between CNF and the PE-foil is useful for preventing drying from driving shrinkage of a CNF film when manufacturing CNF-films (Tammelin Tekla 2013).

Figure 2a, b show photo images of the spun CNF filaments before and after removal from the drum. The filaments were uniform and no visual defects or breaks were observed. The diameter of the yarn was as small as approximately 16 micrometers. SEM imaging was utilized to further study the topography of the filaments. As mentioned earlier, without the oil layer the CNF filament dried into the film form, which broke down due to the adhesion of CNF with the polyethylene foil that does not allow the filament to slide along the surface when it dries. With the oil layer, the filament maintained its initial cross-section shape well, as seen from the SEM image (Fig. 2b). It was expected that with the tested dry spinning method, a circular cross-section is maintained, but the result showed that the actual cross-section had a rectangular shape, most probably due to the shrinking forces that pull the drying filament strongly to the surface of the oiled capstan. Interestingly, when the filament was spun from TEMPO-oxidized CNF, a more flattened filament cross-section was observed, mostly due to the higher water content of TEMPO-oxidized CNF than unmodified CNF. This is evident from the mechanism speculated on above: that is, a drying-driven reshaping of dry-spun CNF filaments when a solid capstan is utilized as a collector.

When the capstan rotates, it generates a moving airfield around the capstan surface that effectively dries the filament. It was observed that a few minutes of rotation time was adequate to fully dry the filament so that it was possible to remove it from the capstan and no further drying-based shrinking was observed. This is a remarkable advantage compared with the currently reported wet spinning methods, where the extended drying steps under external stretching are required to prevent drying-driven shrinking, which lowers the mechanical strength of CNF filaments (Håkansson et al. 2014). Therefore, it can be concluded that the capstan itself prevents the drying-based shrinking of prepared CNF filaments effectively.

Effect of the spinning conditions on the strength profile of the dry-spun CNF filaments

The fiber orientation influences remarkably the strength of a CNF filament (Håkansson et al. 2014). In the investigated dry-spinning method, the ratio between the jet flow and the surface velocity of the capstan opens a new venue to control the orientation of the filament. The filament spinning was carried out with a short linear nozzle (length 8 mm) with the limited hydrodynamic orientation capability. Therefore, the increase in the orientation was also achieved with the collector capstan. It can be seen from Fig. 3 that if the stretch ratio is below 1, the CNF filament's strength was decreased 17 % compared to the strength at a stretch ratio of 1 (tensile strength was 120 and 145 MPa with stretch ratios of 0.7 and 1, respectively).

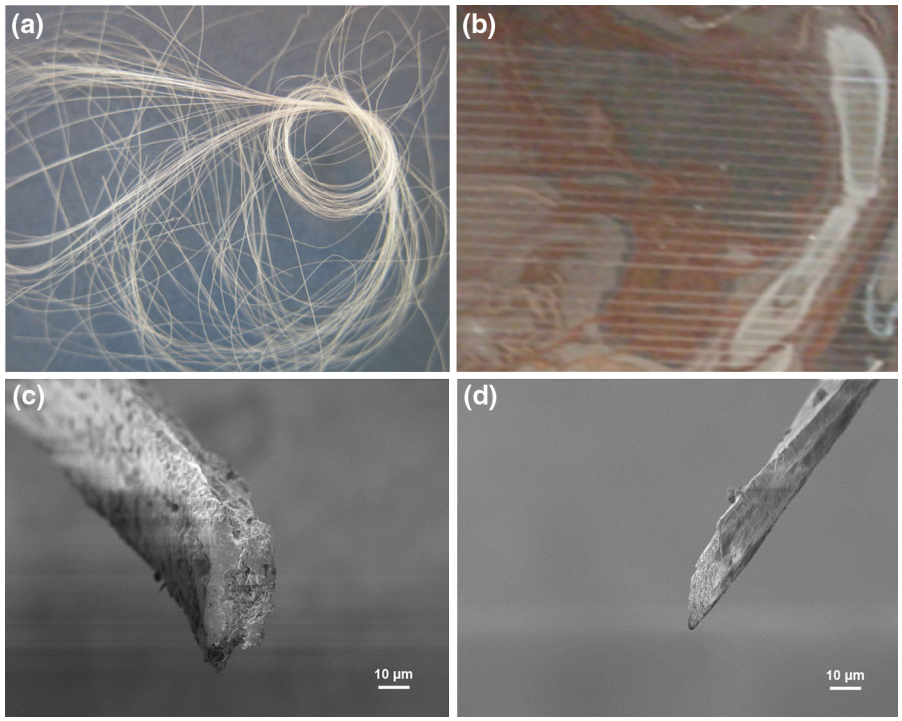

Fig. 2 Photo image of dry spun CNF-filaments **a** after and **b** before removing from the drum (capstan) and SEM images of the dry-spun **c** unmodified and **d** TEMPO-oxidized CNF filaments

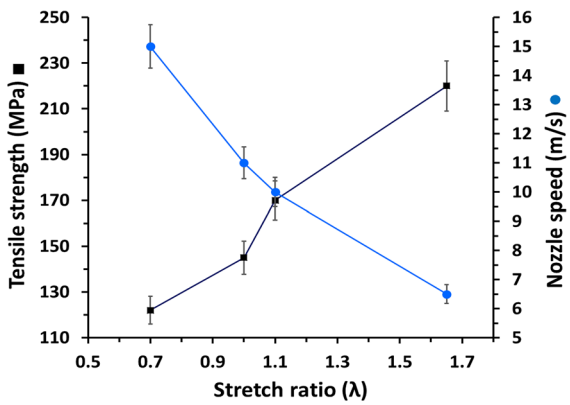

Fig. 3 The tensile strength of CNF filaments as a function of the stretch ratio. The adequate nozzle speeds are presented also. Spinning condition: unmodified CNF consistency 3 % and surface speed 11 m/s. Note, the nozzle speed is marked with "*filled circle*" and tensile strength with "*filled square*". The deviation of nozzle speeds was estimated to be 5 %. The standard deviation of tensile strengths was calculated from seven parallel measurements

When the stretch ratio was above 1, the strength of the CNF filaments increased remarkably. Only a 10 % increase in the stretch ratio increased the tensile strength of the CNF filament over 17 % from 145 to 170 Mpa. The highest strength value (220 MPa) was observed when the stretch ratio was 1.7 (maximum value to the laboratory instrumentation used in this study). However, it is expected that stretching ratios higher than 1.7 can also be utilized to further increase the mechanical properties of the prepared filament. In this study, SEM was utilized to investigate the orientation of the CNF filament. However, it was recognized that it was challenging to observe individual nanofibers due to the limited contrast of SEM-images. Fibril orientation measurements will be carried out in future.

Estimation for limits for spinning speeds

In the ideal case, both the high jet speed and high stretch ratio should be used in the CNF filament manufacturing if the best fiber alignment is targeted. It was noticed that a CNF consistency above 3 wt% with an inner nozzle diameter of 108 µm does not allow for higher jet speed than 16 m/s before the nozzle gets clogged. The 16 m/s jet speed corresponds to over

2000 rpm for the utilized capstan, with a stretch ratio of 1.7. When the consistency of the CNF gel was decreased from 3 to 1.64 wt%, the operation window of the stretch ratio was adversely shifted to the lower end. Therefore, the higher stretch ratio would simply cause fiber breakage, which in turn suggests higher CNF consistencies. Thus a compromise has to be made between the CNF consistency, nozzle speed, and stretch ratio. It can be concluded that the investigated dry-spinning method for manufacturing CNF filaments offers a valuable addition to the traditional wet-spinning methods. However, further research is required to investigate the effects of nozzle geometry, environment humidity, and drying speed.

Conclusions

A new process to manufacture cellulose nanofiber filaments was demonstrated. CNF was extruded through a fine nozzle onto a moving low friction surface at a speed as high as 11 m/s. The non-adhesive surface was manufactured by coating a polyethylene covered capstan with a thin layer of sunflower oil. The wet filament was air dried on the slippery surface to form ribbon like nanofiber yarns. The stretch ratio between the jet and the collector capstan can be utilized to fine tune the orientation of CNF in the CNF-filament.

Acknowledgments The work started as part of the Design Driven Value Chains in the World of Cellulose project (DWOC) funded by Tekes the Finnish Funding Agency for Innovation and continued through VTT's internal project funded with the aid of a government grant. The authors appreciate the help from Panu Lahtinen and Minna Hakalahti for providing the nanocellulose samples, as well as for valuable discussions with Jari Vartiainen and Heikki Pajari about slippery surfaces.

References

Cook JG (1984) Handbook of textile fibres: man-made fibres. Elsevier, Amsterdam

Eichhorn SJ, Dufresne A, Aranguren M et al (2010) Review: current international research into cellulose nanofibres and nanocomposites. J Mater Sci 45:1–33

Håkansson KMO, Fall AB, Lundell F et al (2014) Hydrodynamic alignment and assembly of nanofibrils resulting in strong cellulose filaments. Nat Commun 5:4018. doi:10.1038/ncomms5018

Hooshmand S, Aitomäki Y, Norberg N et al (2015) Dry-spun single-filament fibers comprising solely cellulose nanofibers from bioresidue. ACS Appl Mater Interfaces 7:13022–13028. doi:10.1021/acsami.5b03091

Isogai A, Kato Y (1998) Preparation of polyuronic acid from cellulose by TEMPO-mediated oxidation. Cellulose 5:153–164

Iwamoto S, Isogai A, Iwata T (2011) Structure and mechanical properties of wet-spun fibers made from natural cellulose nanofibers. Biomacromolecules 12:831–836. doi:10.1021/bm101510r

Klemm D (1998) Comprehensive cellulose chemistry. Fundamentals and analytical methods, vol 1. Wiley-VCH, Weinheim

Nogi M, Iwamoto S, Nakagaito AN, Yano H (2009) Optically transparent nanofiber paper. Adv Mater 21:1595–1598

Paakko M, Vapaavuori J, Silvennoinen R et al (2008) Long and entangled native cellulose I nanofibers allow flexible aerogels and hierarchically porous templates for functionalities. Soft Matter 4:2492–2499. doi:10.1039/B810371B

Lafuma A, Quéré D (2011) Slippery pre-suffused surfaces. Europhys Lett 96:56001

Syverud K, Stenius P (2009) Strength and barrier properties of MFC films. Cellulose 16:75–85

Tammelin T, Hippi U, Salminen, A (2013) Method for the preparation of nanofibrillated cellulose (NFC) films on supports. PCR Int Appl WO2013060934A2

Turbak A, Snyder F, Sandberg K (1983) Microfibrillated cellulose, a new cellulose product: properties, uses, and commercial potential. J Appl Polym Sci: Appl Polym Symp 37:815–827

Walther A, Timonen JVI, Díez I et al (2011) Multifunctional high-performance biofibers based on wet-extrusion of renewable native cellulose nanofibrils. Adv Mater 23:2924–2928. doi:10.1002/adma.201100580

Wong T-S, Kang SH, Tang SKY et al (2011) Bioinspired self-repairing slippery surfaces with pressure-stable omniphobicity. Nature 477:443–447